ANALISYS OF FLOW PATTERNS DURING BOILING OF R-134a AND R-600a IN A MINI TUBE

Jacqueline Biancon Copetti
Rosele Argenta Sodré
Mario Henrique Macagnan
Mechanical Engineering Graduate Program-Universidade do Vale do Rio dos Sinos
Av. Unisinos, 950 93028-000 São Leopoldo, RS, Brazil
e-mails: jcopetti@unisinos.br, rosele_asodre@yahoo.com.br, mhmac@unisinos.br
Jeferson Diehl de Oliveira
Mechanical Engineering Graduate Program – Universidade Federal de Santa Catarina
jeferson.physis@hotmail.com

Abstract. *This paper presents an experimental and theoretical study of flow patterns during the flow boiling of refrigerants R-134a and R-600a, in a 2.6 mm ID tube. It is carried out from a database of experimental heat transfer coefficients obtained during flow boiling of these refrigerants considering heat fluxes between 10 and 160 kW/m², mass velocities between 188 and 930 kg/m² s and vapor qualities from 0 to 0.9, for the saturation temperature of 22 °C. A comprehensive review on the flow pattern maps, their evolution and application, is presented, as well as the analysis of the use of the maps to the experimental conditions of this work. This analysis is completed by a comparison with the flow images obtained during tests using a high-speed video camera. The results of heat transfer coefficients for different points on the tube perimeter are also used to help in the characterization of the flow patterns transition. It has been found that the predominant patterns for these fluids and dimensions are elongated bubble, slug, churn and annular. Stratified flow pattern was not observed in any of the tests. For the refrigerant R-600a the transition between patterns always happens in lower vapor qualities than for R-134a, at the same mass velocity.*

Keywords: *flow patterns, boiling in mini tube, heat transfer coefficients, R-134a, R-600a*

1. INTRODUCTION

Flow boiling in narrow channels can absorb larger amounts of thermal energy relative to single-phase flow, through its latent heat of vaporization. The improvement of heat transfer coefficient with a reduction of channel size has been reported in literature, however the results show numerous discrepancies regarding the effects of vapor quality, mass velocity, saturation pressure and heat flux on the heat transfer coefficient, as analyzed by Ribatski (2012). Furthermore, significant differences in two-phase transport phenomena have been verified between microscale and macroscale geometries and these differences limit the ability to predict heat transfer performance in small channels.

A literature review was undertaken considering experimental studies on boiling in channels smaller than 5 mm in diameter and the range of conditions is similar to the one considered in this work. The studies show the heat transfer coefficient behavior under different conditions during boiling. Tran *et al.* (1996) studied R-12 in a 2.46 mm circular tube and observed the heat transfer dependence of heat flux, but the effects of mass velocity and vapor quality were negligible. The same tendency had already been reported by Lazarek and Black (1982) and Wambsganss *et al.* (1993) with R-113 boiling in a 3.1 mm and 2.92 mm tubes, respectively. However, the results shown by Yan and Lin (1998) and Lin *et al.* (2001) demonstrated that the effects of mass velocity and vapor quality are also important. The heat transfer coefficients obtained from experiments carried out by Lin *et al.* (2001) with R-141b in 1.3 to 3.69 mm channels showed similar trends to those observed in the macroscale. The heat flux was important only in the low quality region $(X < 0.4)$ and the heat transfer coefficient increased with the increase in vapor quality until a point when the coefficient decreased gradually, but the inflection point in the vapor quality range was also heat flux dependent. Saitoh *et al.* (2005) analyzed the effect of tube diameter on boiling heat transfer of R-134a with heat fluxes in the range of 5 to 39 kW/m² and mass velocities between 150 and 450 kg/m² s. For a 3.1 mm ID they found a clear dependency of the heat transfer coefficient on both heat and mass flux, unlike for the 0.51 mm tube, where they observed the effect of heat flux only. These authors suggested that the contribution of forced convection to the boiling heat transfer decreases with decreasing tube diameter, while dryout occurred at lower values of vapor quality in smaller channels as the effect of confinement becomes important.

With decreasing channel size, the dominant mechanisms in macrochannels, are now less important. In the transition from macro to micro behaviors, bubble confinement within the channel and the importance of different forces that can act, like gravitational, inertial and surface tension must be considered. For example, while gravity plays an important role in macroscale, it has less effect in microscale due to the contrasting effect of surface tension, consequently modifying the flow patterns.

Studies about flow pattern in microscale have indicated the suppression of the stratified and stratified-wavy flow regimes, the convergence of slug and plug flows into the elongated bubble flow regime, and early transition of elongated bubble flow to churn-annular or annular flow regime with respect to vapor quality (Revellin and Thome, 2007; Arcanjo *et al.*, 2010).

The investigation of air–water and R-134a in small circular channels from 1 to 3 mm by Yang and Shieh (2001) concluded that surface tension is an important parameter in the determination of flow regimes in small scale channels. Shiferaw *et al.* (2007) studied the dependence of flow boiling heat transfer of R-134a in a 2.01 mm and 4.26 mm diameter channel for different mass fluxes and concluded that the flow regime transition boundaries for slug/churn and churn/annular shifted significantly for lower vapor qualities as the mass flux increases. Thus, demonstrating the dependence of mass velocity on flow regime transitions. The heat transfer coefficient increased with heat flux and saturation temperature, but it remained constant in the vapor quality range from 0.4 to 0.5 in low heat fluxes. For the 2.01 mm tube, this range moved down to 0.2 to 0.3 of vapor quality.

More recently, Tibiriçá and Ribatski (2010) and Ong and Thome (2009), presented a comprehensive study of the flow boiling in small tubes for different refrigerants, including the R-134a. The first work examined the influence of mass velocity from 100 to 700 kg/m²s and heat flux from 5 to 35 kW/m² and the authors found that the heat transfer coefficient increased with the mass velocity and vapor quality except for mass velocities below a threshold of 200 kg/m²s, which experimented a premature and smooth decrease with increasing vapor quality. Also, the heat transfer coefficient increased with heat flux independently of the fluid or mass velocity range. In the second work, Ong and Thome (2009) analyzed the heat transfer coefficient behavior for different refrigerants and it was associated to flow regime transition for different vapor qualities. They concluded that convective boiling seems to dominate at higher vapor qualities in the annular flow, and in the bubbly regime, at low vapor qualities, the heat transfer coefficient depends on heat flux. As the mass velocity increases the transition to annular flow occurs at lower qualities. The flow regimes observed in their experiments were: bubbly flow with buoyancy effects, elongated bubble (slug) flow, churn, annular, and mist flow at very high vapor qualities. No stratified flows were observed.

The authors of this work previously published the data of heat transfer and pressure drop for boiling of R-134a (Copetti *et al.*, 2011) and R-600a in a 2.6 mm tube (Copetti *et al.*, 2013) and compared the data of heat transfer coefficient with different correlations and the errors reached around 50%. Considering these results is therefore advisable to explore more the data behavior and their relation with flow patterns, which permits the development of physically based heat transfer models, including flow pattern in small scale channels, the refrigerants characteristics and temperature. Moreover, the hydrocarbon isobutane (R-600a) has shown be an interesting refrigerant for use in small tubes, due to your properties and thermal-hydraulic behavior.

2. EXPERIMENTAL DATA BASE OF HEAT TRANSFER COEFFICIENTS

An experimental facility was developed to investigate flow boiling and pressure drop of refrigerants in a horizontal mini-channel according to the Fig. 1 and more details of this facility were presented in Copetti *et al.* (2013). The experimental system consists of a loop that provides controlled fluid mass velocity and it was designed to test different fluids under a wide range of flow conditions. The main part of the loop has a pre-heater section (PHS), the test section (TS) and the flow visualization section (VS) and the secondary part have a condenser, a refrigerant reservoir, a liquid refrigerant vessel, a volumetric pump and a subcooler, that guarantee the fluid condensation, saturation temperature and pressure control, besides the conditions and stability of flow. The PHS establishes the experimental conditions entering the test section immediately downstream and then initial vapor quality is defined this way. The TS consists of a horizontal stainless steel tube with effective length of 185 mm, 2.6 mm ID and absolute internal roughness of 2.05 μm. The tube is uniformly heated by direct application of an electrical current in the tube wall, the intensity of which is controlled by the power supply. Downstream of the TS there is a VS with a 158 mm length glass tube with the same test section internal diameter. The flow images and videos are registered by a high velocity digital camera (3000 fps in the maximum resolution).

The data of temperature and pressure in the inlet and outlet of PHS and TS were registered. The wall temperatures were measured by thermocouples directly fixed at five axial positions along the TS tube, with four thermocouples at each position, each one separated by 90º from the other, as indicated in Fig.1. The pump flow rate is controlled by a frequency inverter and a bypass line downstream of the pump, controlled by a needle-valve, is used to set precise flow rates. The pressure transducers, thermocouples, mass flow and power meters were connected to an acquisition data system composed of a multimeter (Agilent, model 34970A) and LabView software control the measurements, recorded the data and make the data reduction with a RefProp interface. The uncertainties of measured parameters are 0.5 ºC for temperature, 0.1 kPa for absolute pressure, 0.045 kPa for differential pressure and 0.2 % for mass velocity.

The Tab. 1 list the range of operational conditions considered in the boiling tests for the two refrigerants.

Table 1. Test conditions.

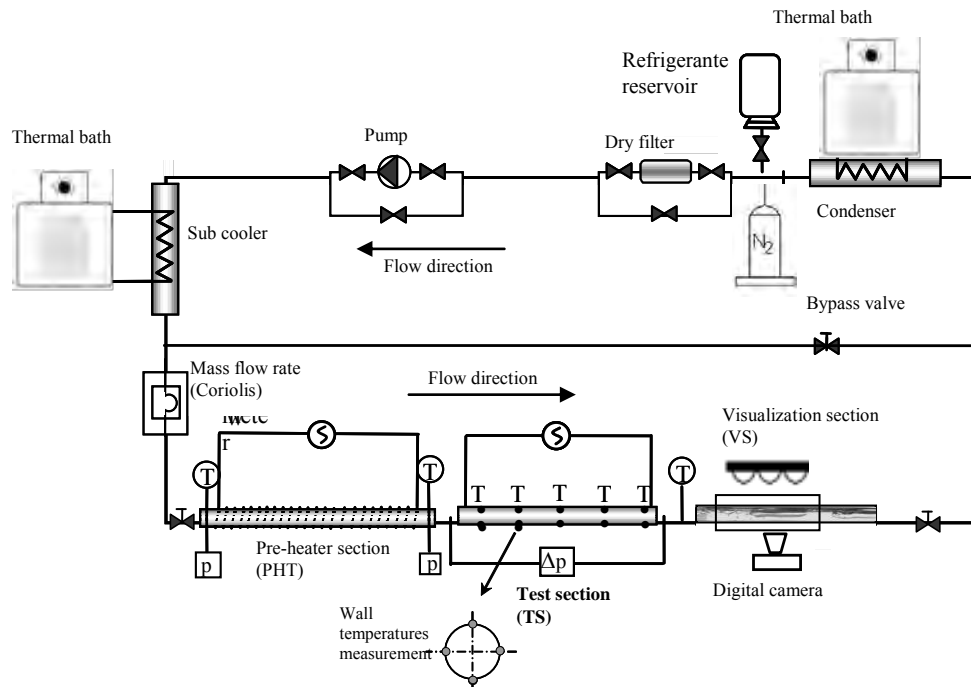| Refrigerants	R-600a	R-134a
Test section heat flux, q" (kW/m²)	33, 47, 67, 100, 120 and 160	10, 20, 33, 47, 67, 87 and 100
Mass velocity, G (kg/m²s)	188, 240, 280, 370 and 440	240, 440, 556, 740, 930
Saturation temperature, Tsat (°C)	22	22 and 12

Figure 1. Schematic view of the experimental facility.

2.1 Some results of average heat transfer coefficient behavior

The analysis of average heat transfer coefficient behavior with vapor quality, at different boiling conditions, is shown in Figs. 2, 3 and 4, and some remarks are listed below:

- The influence of heat flux was observed in the low quality region, for both refrigerants. The coefficient increases with increasing in heat flux, however in the high vapor quality region, for high mass velocities, this influence tended to disappear and the coefficient decreased (Fig. 2). This behavior is related to the flow pattern transitions, as can be seen later.
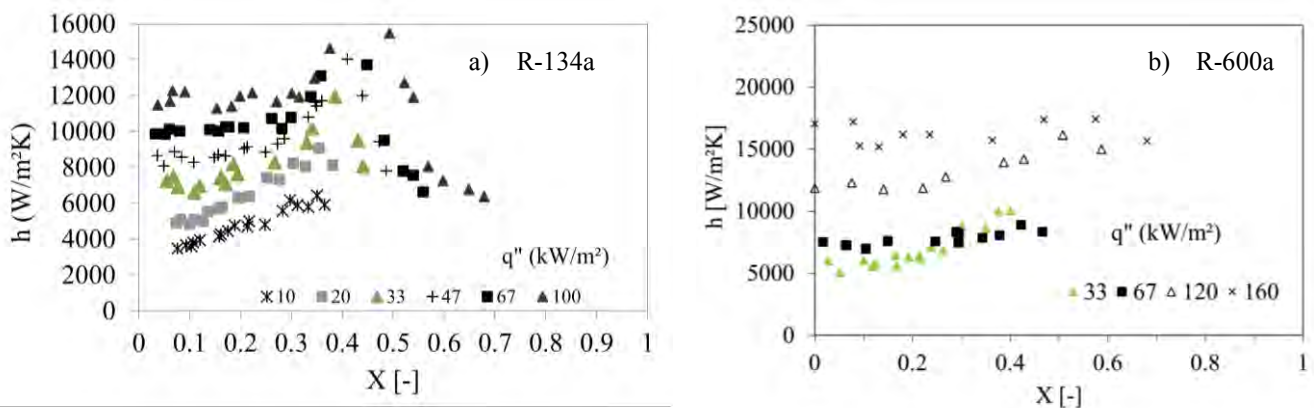

Figure 2. Effect of heat flux on the heat transfer coefficient for *Tsat* = 22 ºC and the two refrigerants: (a) R-134a and *G* = 440 kg/m²s; (b) R-600a and *G* = 280 kg/m²s.

J. Copetti, R.A. Sodré, M.H.Macagnan, J.D. Oliveira
Boiling flow patterns in mini tube

- The influence of mass velocity on the heat transfer coefficient was also detected in the tests, but for the highest heat flux value the heat transfer coefficient was almost independent of mass velocity (Fig. 3).
- When comparing the refrigerants R-600a and R-134a, the same behavior was observed with respect to the effect of different parameters, however the former showed higher heat transfer coefficients for similar operation conditions (Fig. 4a).
- The heat transfer coefficient increased with decreasing saturation temperature (Fig. 4b). Properties such as surface tension, density and liquid viscosity, increase with decreasing temperature, thus explaining the coefficient behavior with temperature.
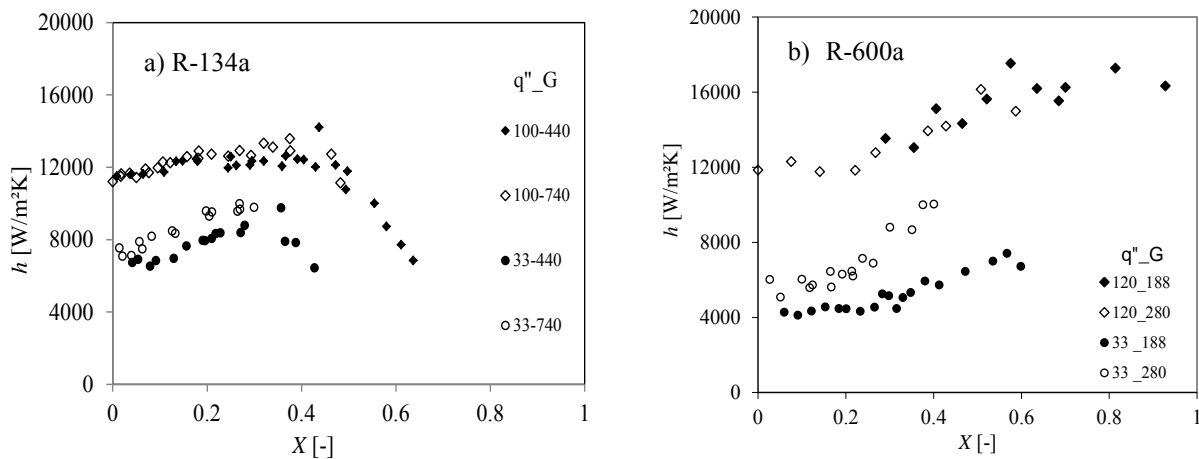
Figure 3. Effect of mass velocity on the heat transfer coefficient for $Tsat$ = 22 ºC and the (a) R-134a and (b) R-600a.

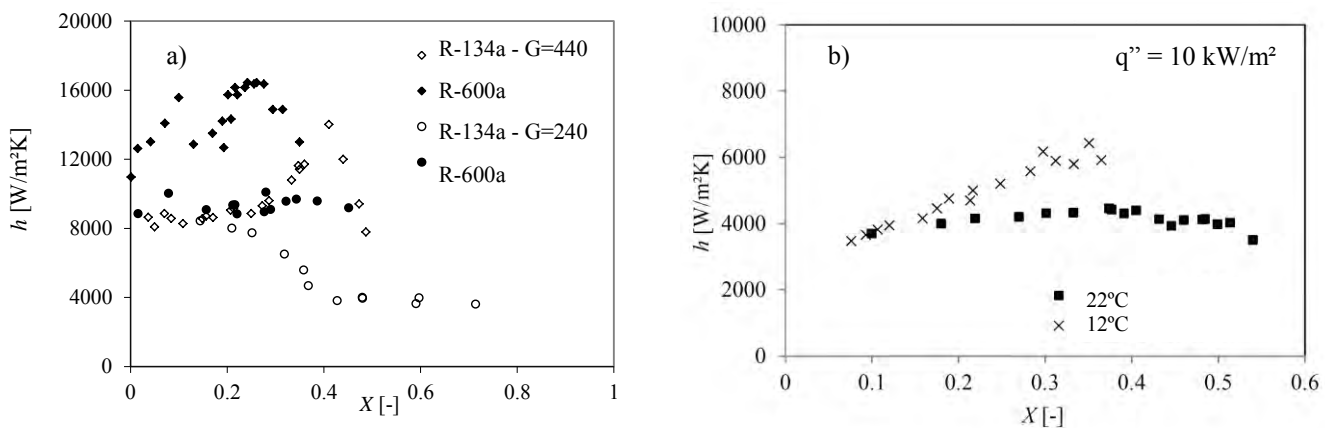Figure 4.(a) Comparison of heat transfer coefficient of R-600a and R-134a for heat flux of 47 kW/m²; (b) Effect of saturation temperature on R-134a heat transfer coefficient for G = 440 kg/m²s.

In Table 2 the properties of R-134a and R-600a are presented to allow the comparison of different heat transfer behavior. The lower viscosity (μ) and higher thermal conductivity (k) of R-600a contributed positively to the heat transfer coefficients higher than those of R-134a, confirming the results shown in Fig. 4a.

Table 2. Comparison of properties for the refrigerants for saturation temperature of 22 °C.

Refrigerant	p (kPa)	pr (kPa)	ρ_f (kg/m³)	ρ_g (kg/m³)	k_f (10^{-3} W/mºC)	k_g (W/mºC)	μ_f (10^{-6}Pa.s)	μ_g (10^{-6}Pa.s)	i_{fg} (kJ/kg)	σ (10^{-3} N/m)
R-134a	607.89	0.15	1218	29.54	82.42	13.53	202.28	11.57	180.51	8.48
R-600a	320.72	0.088	553.69	8.38	90.10	16.51	155.09	7.42	332.42	10.45
Air-Water	101.3	-	997.4	1.197	589.3	25.28	858.3	18.30	-	72.1

2.2 About the flow patterns and maps - comparison

Flow pattern maps are being proposed to characterize two phase flow, however the majority is based in observations for channels with diameters higher than 10 mm, considered macrochannels. In horizontal tubes in this scale, the patterns in general are identified as bubbly, plug, stratified, slug and annular and are associated to different forces as inertia, surface tension, shear, gravity and momentum. Kandlikar (2010) analyzed the importance of these forces associated to evaporation in the interface for mass velocity of 200 kg/m²s. In macro scale the flow patterns suffer significant influence of gravity forces and inertial forces, nevertheless with reduction in channels diameter the surface tension force replaces gravity. But for diameters around 3 mm the author observed equilibrium between these three forces, inertial, surface tension and gravity. This threshold of 3 mm is considered by some authors (Bertsch *et al.*, 2009; Thome *et al.*, 2004; Cheng and Wu, 2006), a limit for transition from macro to micro scale.

In the characterization of transitions in flow patterns are used parameters like superficial velocities, mass velocity, void fraction and vapor quality.

Taitel and Dukler (1976) were the pioneers, when developed a method to predict the patterns for adiabatic two phase flow based in physical mechanisms using dimensionless parameters. Many flow pattern maps were presented subsequently considering the base of these authors.

Wojtan *et al.* (2005) proposed a flow pattern map based in dynamics void fraction measurements using optical technique for flow boiling of R-22 and R-410A in tubes of 13.8 and 8 mm diameters, mass velocity from 70 to 700 kg/m²s and heat flux in the range of 2 to 57.5 kW/m². The map is based in the analysis the liquid-vapor interface during stratified flow and the study of transition from annular to mist flow. From heat transfer measurements, the flow was classified in eight patterns: Slug (Sl), Slug and Stratified-Wavy (Sl+SW), Stratified (S), Intermittent (I), Annular (A), Dryout (D) and Mist (M). The new transition curves were introduced: A-D and D-M; Sl; Sl+SW and SW. It was observed the influence of mass velocity on flow regime transitions. For lower vapor quality, the transition curves go up with increasing mass velocity, but the effect becomes less significant as the vapor quality increases.

In this work our data base with images and videos, was analyzed with this map, although the experiments were carried out in a tube with smaller diameter. Figure 5 shows the maps for R-134a and two heat fluxes, q" = 33 kW/m² (Fig. 5a) and q" = 100 kW/m² (Fig. 5b). According the heat flux increases is possible to notice the difference in the inclination of curves, the decreasing in the extension of annular (A) region and the increase of dryout (D) and mist (M) regions. The results were compared with the heat transfer coefficient, h, behavior in Figs. 2a and 3a and is possible to verify the decreasing of heat transfer coefficient for the smaller heat flux, q" = 33 kW/m², and mass velocity, G = 440 kg/m²s, agreeing with the transition to annular pattern in the map in Fig. 5a (X $\cong$ 0.35). For the same heat flux, but higher mass velocity, G = 740 kg/m²s, the transition to annular occurs to smaller vapor qualities (X $\cong$ 0.3). Then it is possible to observe in Fig. 5a that flow patterns identified by images are in the intermittent region, even the slug and annular patterns. For the upper heat flux, q" = 100 kW/m², the same behavior for heat transfer coefficient with vapor quality was observed for mass velocities of G = 440 kg/m²s and 740 kg/m²s (Fig. 3a), the transition to annular flow occurs a smaller vapor qualities as the mass velocity increases (X $\cong$ 0.4 for 440 kg/m²s and X $\cong$ 0.3 for 740 kg/m²s). This result is also possible to see in the map of Fig. 5b, but for these conditions the flow pattern identified was almost entirely annular and in the map of Fig. 5b the data are in dry out region.
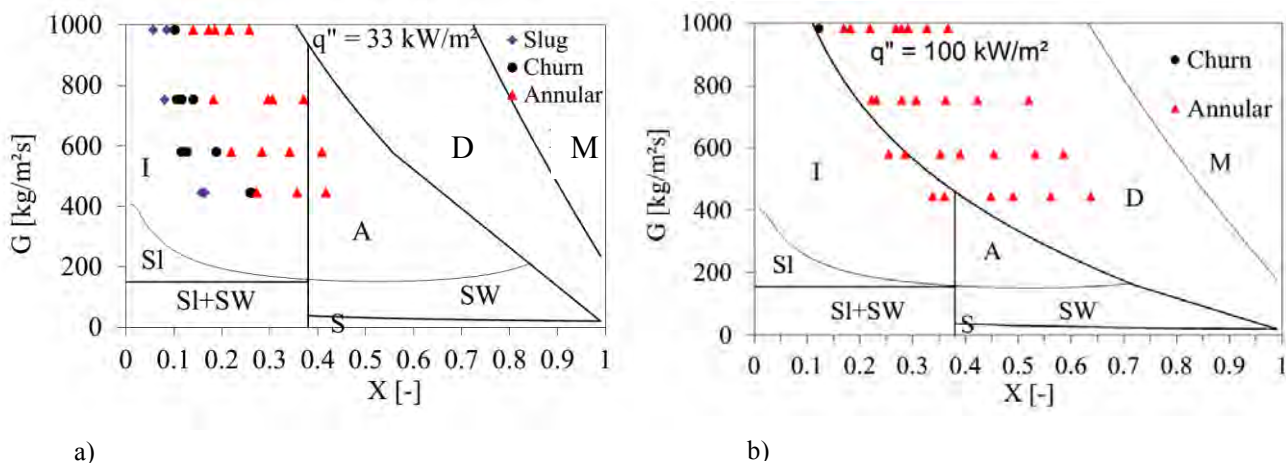

a)   b)

Figure 5. Two-phase flow pattern and transition lines of Wojtan *et al.* (2005) for R-134a at Tsat = 22 °C in a 2.6 mm ID tube and (a) q"=33 kW/m² and (b) q"=100 kW/m².

The flow pattern map for R-600a is shown in Fig. 6 for heat fluxes q" = 33 and 120 kW/m² and mass velocities smaller than for R-134a. The results for h versus X (Figs. 2b and 3b) show a similar behavior of R-134a. In Fig. 6a the map for q"=33 kW/m² it is possible to see slug pattern in the intermittent region and in Fig. 6b with higher heat flux the flow characterize as churn and annular in the map are in dryout region. For q"= 33 kW/m², Fig. 3b, the coefficient increases for entire range of vapor qualities, only at the end of the curve, for G = 188 kg/m²s, is observed start of coefficient decreasing and this point in the map of Fig. 6a is very close to the annular-dryout pattern transition. For greater heat flux, q" = 120 kW/m², Fig. 6b, the coefficient h is increasing, since the flow is in the dryout region. In this heat flux and G = 188 kg/m²s is possible to see the decreasing of h in X > 0.8, and in the map this condition is in mist region. It is important to point out that for greater mass velocity, the decrease in the coefficient h occurs in minor vapor quality, also see Fig. 4a. Furthermore, in comparison of curves and maps for the two refrigerants, the transition curves of R-600a are displaced to the minor vapor qualities sometimes anticipating the transition between flow patterns.

The stratified flow pattern and its subdivisions are not observed for our experimental data.
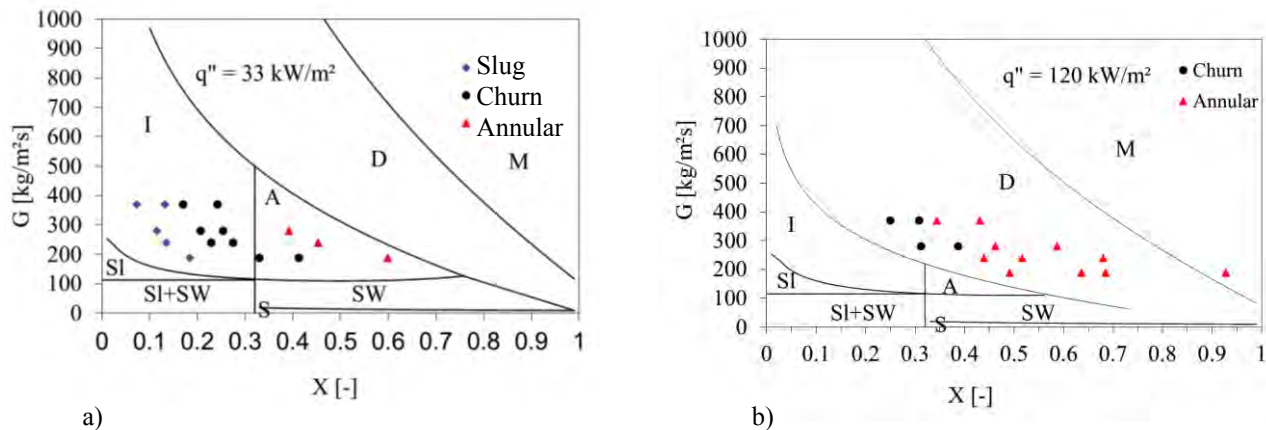

Figure 6. Two-phase flow pattern and transition lines of Wojtan et al. (2005) for R-600a at Tsat = 22 ºC and (a) q"=33 kW/m² and (b) q"= 120 kW/m² for 2.62 mm channel.

In micro scale most of the studies were focused on flow pattern transitions for air-water, but with refrigerants the results can be quite different considering the differences in the properties like surface tension and viscosity, as shown in Tab. 2. The surface tension, σ, for air-water is around 8 times higher. Moreover, flow maps are developed for specific conditions and thus they cannot be generalized methods.

The first flow patterns map for small channels was proposed by Barnea et al. (1983) including surface tension effects in the transition between patterns and analyzed the gravity forces influence. They characterize the flow pattern as: dispersed flow (bubbly and mist flows), stratified flow (smooth + wavy), intermittent flow (slug, elongated bubbles and churn) and annular flow. Ulmann and Brauner (2007) identified the relevant dimensionless variables to explain the transition to annular flow in micro scale and the wall wetting effects for air-water flow in 1 mm pipe. According to the authors, reducing the pipe diameter the stratified flow region shrinks, and may be limited to only a small region of very low liquid flow rates (and relatively high gas flow rates), but in this flow rate range the distinction between stratified and annular flow is ambiguous. Felcar et al. (2007) worked with air-water database and proposed modifications in the method of Barnea and coworkers to predict the transition from stratified and intermittent to annular flow in channels smaller than 3 mm. They consider surface tension and contact angle effects, which are negligible in larger tubes, by adding a new parameter as a function of Eötvos number, Eo, for the capillary and gravitational effects, and Webber number, We, for inertial and surface tension effects. The effects of wettability were neglected in the Eo number. Revellin and Thome (2007), developed an optical measurement technique, with micro lasers and photodiodes was used to characterize the flow regimes, complemented with flow pattern videos acquired high speed camera. The new flow pattern map proposed was based on observations for R-134a and R-245fa boiling in 0.509 and 0.790 mm channels. They determined the frequency of bubbles, their coalescence rates and lengths, as well as their mean two-phase vapor velocity. The pattern map for evaporating flow in microchannels was proposed with an isolated bubble (IB) regime, coalescing bubble (CB) regime, annular (A) regime and mist (M) flow regime.

As the channel diameter decreases the bubble is confined and then elongated. Kew and Cornwell (2001) proposed the Confinement number, Co, which represents the ratio of capillary length to the channel diameter and can serve to delineate the transition from macrochannel to microchannels flows, because this number trends to increase according the channel diameter decreases. The authors suggested the threshold of Co = 0.5. Then for the refrigerants and conditions of our experiments for R-134a the number Co = 0.325, a mini channel flow, and for R-600a, Co = 0.533, a microchannel flow. This result is also supported to the higher surface tension of R-600a than R-134a, how is possible to verify in Tab. 2.

Ong and Thome (2011) published a study that focuses on investigating the transition from macro to microscale during flow boiling in small scale channels of three different sizes (1.03, 2.20 and 3.04 mm diameter) with three different refrigerants (R134a, R236fa and R245fa) over a range of saturation conditions to investigate the effects of channel confinement on two-phase flow patterns and liquid film stratification in a single circular horizontal channel. The high speed image processing of flow visualization videos aided define the macro-to-microscale transition in two-phase flow. Based on the work of Revellin and Thome (2007) an improved flow pattern map has been proposed by the authors that includes new dimensionless numbers for considering the effects of gravity, inertia and surface tension and the determination of the flow patterns transitions. The model considers the transition to macroscale slug/plug flow at a confinement number of Co = 0.3 - 0.4 and, from the top/bottom liquid film thickness comparison results, the authors concluded that the gravity forces are suppressed and overcome by the surface tension and shear forces when Co→ 1.0 (microscale).

The flow pattern map considers transitions from Isolated Bubble (IB) to Coalescent Bubble (CB) to Annular (A) (smooth and wavy) flow for microchannels. For channels with major scale, the IB flow pattern is replaced by Plug/Slug (PS) pattern that constitutes a long vapor bubble separated by liquid plugs that exhibit strong buoyancy effects and a thick stratified layer of liquid at the bottom of the elongated bubbles. According the authors wavy annular flow is similar to the churn – annular flow regime in macroscale. Then, considering the data base of this work the maps were built and the results are shown in Fig. 7. In these figures the flow images recorded with the high speed camera during the tests for different mass velocities and vapor qualities are included. They are useful to identify the flow patterns. The specific condition of each image is marked in the graphs.

In these maps are plotted the measures for all heat fluxes, since it is found that the heat flux does not significantly alter transition curves, unlike what happened with map of Wojtan *et al.*(2005).
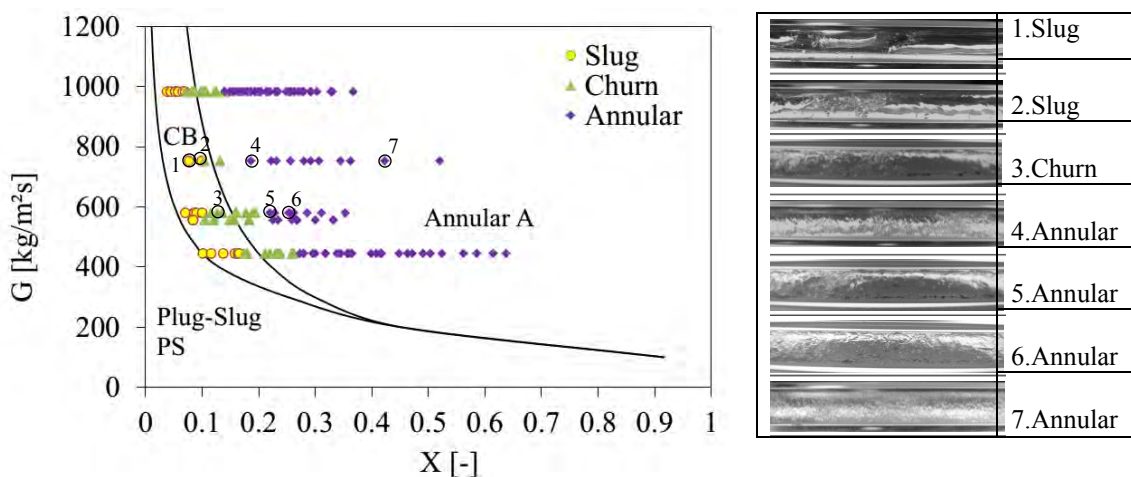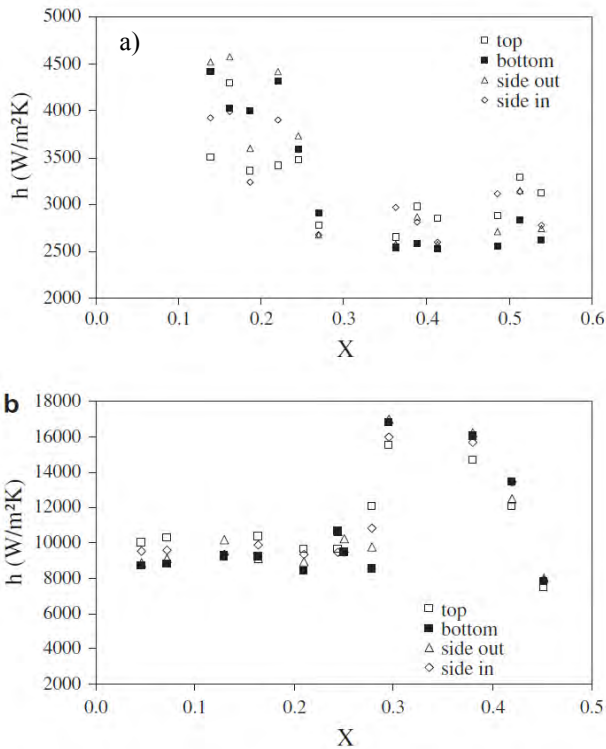

a) R-134a
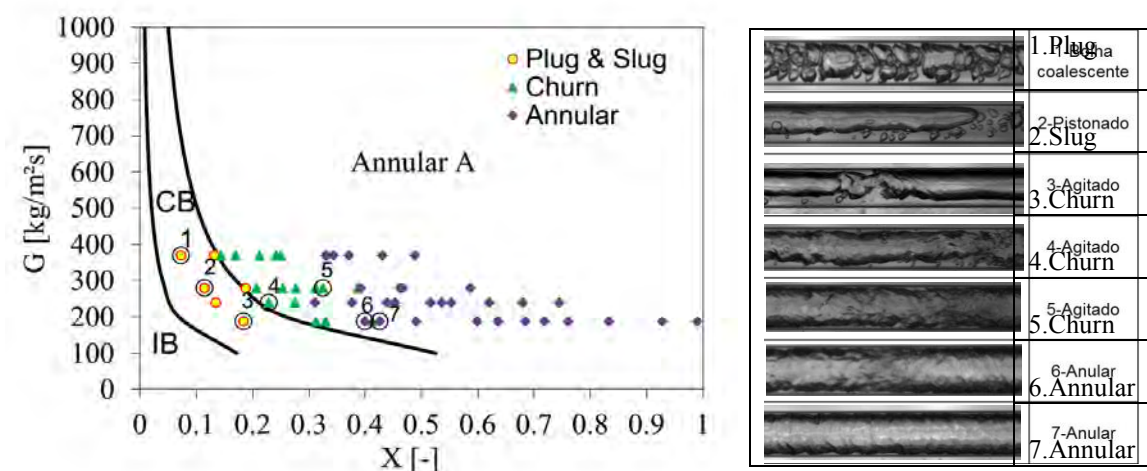
b) R-600a

Figure 7. Two-phase flow pattern and transition lines by Ong and Thome (2011) and images for (a) R- 134a and (b) R-600a at saturation temperature of 22 ºC and for 2.62 mm channel.

The Plug/Slug (PS) was considering for R-134a (Co = 0.325) and for R-600a (Co = 0.53) this region, according the map doesn´t exist (Figs. 7a and 7b, respectively). The annular (A) flow regime gradually expands and spans over a wider range of vapor qualities with increasing mass velocity. The CB/A transition is reached when the inertia force dominates over the surface tension force, promoting coalescence to form a continuous vapor core. The earlier CB/A transition trend is associated to the less dominant surface tension forces (IB and PS) compared to inertia, reducing the ability of the flow to keep the liquid slug hold up between the vapor bubbles. Then in annular regimes the shear forces gain domain.

The results in Figs. 7a and 7b, in accordance with previous Figs. 2 and 3, for higher mass velocity the vapor quality for transition CB/A occurs at lower values of vapor quality. However, for both refrigerants the plug and slug flow patterns identified, are in the coalescing bubble (CB) region of the map, independent of mass velocities. The analysis of the maps in Figs. 7a and 7b indicate that the curves transition could be the curves displaced to the right, in direction to vapor quality increases.

An analysis was carried out with respect to measurements of the wall temperature distribution along to the tube perimeter (as indicated in the Fig. 1). The results of the heat transfer coefficient at the four locations (top, bottom, side_outer and side_inner) are shown in Fig. 8a and b.

In Fig. 8a, for the lower mass velocity, G = 240 kg/m²s, the top is found to be the lowest up to X = 0.3, compared wi is due to vapor in contact with the upper portion of the tub distribution that can be related to the unsteadiness of liquid transfer coefficient distribution above X = 0.3 may corresp occurs. For the case of higher mass velocity, G = 440 kg/m² the heat transfer coefficient increases along the tube and its the top heat transfer coefficient is higher than bottom and condition is inverted to quality over 0.3, where the bottom h transition to annular flow.
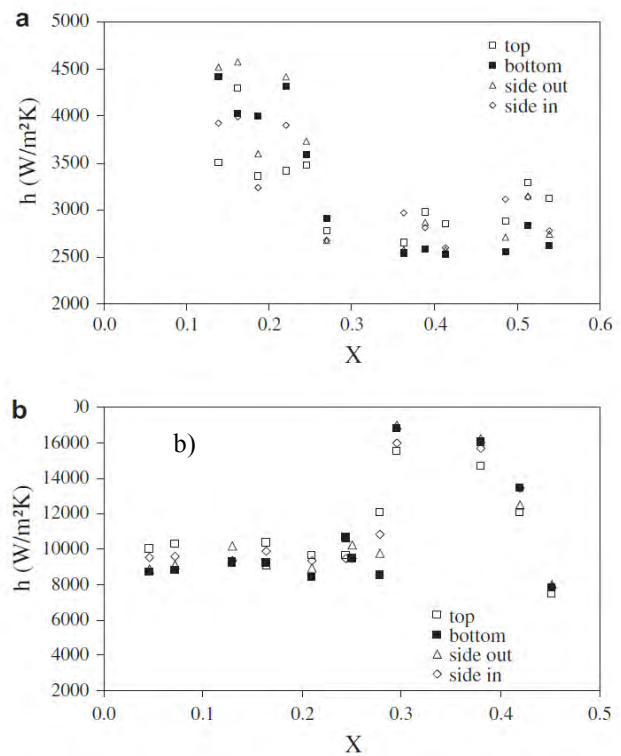
g. **4.** Heat transfer coefficient distribution along to the tube diameter for at = 22 °C and different mass velocity and heat flux: (a) $G = 240$ kg/m² s and = 10 kW/m²; (b) $G = 440$ kg/m² s and $q'' = 67$ kW/m².

s. The R-600a yields the lowest IB/CB and CB/A vapor vior of heat transfer coefficient comparison for both efrigerants. The surface tension of R-600a exceeds the values result in an increased degree of expansion of the almost double of R-134a and this property is relating to ne IB/CB diabatic. Other important characteristic of
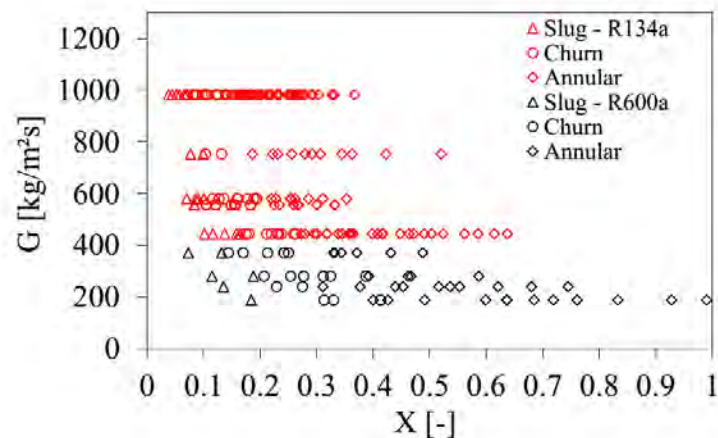
g. **4.** Heat transfer coefficient distribution along to the tube diameter for at = 22 °C and different mass velocity and heat flux: (a) $G = 240$ kg/m² s and = 10 kW/m²; (b) $G = 440$ kg/m² s and $q'' = 67$ kW/m².

Figure 9. Flow patterns for refrigerants R-134a and R-600a at saturation temperature of 22 ºC.

3. CONCLUSIONS

Experimental results for the flow boiling of R-134a and R-600a in a horizontal small tube under the variation of mass velocity, heat flux, saturation temperature and vapor quality were presented. The behavior of the local heat transfer coefficient was investigated and the following conclusions could be drawn from this study:
- In the low quality region, it was observe the influence of heat flux on the heat transfer coefficient. In the high vapor quality region, for high mass velocities, this influence tended to vanish, and the coefficient decreased.
- The influence of mass velocity in the heat transfer coefficient was detected in most tests for a threshold value of vapor quality, which was higher as the heat flux increased. For higher heat flux the heat transfer coefficient was nearly independent of mass velocity.
The flow patterns visualization during the tests was identified for both refrigerants indifferent conditions of heat fluxes and mass velocities and basically were slug, churn and annular. Elongated bubbles flow was verified only for high mass velocity and very low vapor quality.
Two flow pattern maps were analyzed with these data base of heat transfer coefficient behavior at various vapor qualities and images of flow patterns. For the Wojtan et al. (2005) map for macro channels, the curve transitions not agree with the data and the stratified flow it was not observed. With the Ong and Thome (2011) map for mini and microchannel the fit is better. The trends of transition curves correspond but they should be corrected, displacing them to the lower vapor qualities. Isolated bubble regime (IB) was not observed. For higher mass velocity and heat flux the vapor quality for transition CB/A occurs at lower values of vapor quality. The R-600a yields the lowest IB/CB and CB/A vapor quality transition when compare with R-134a behavior.

4. REFERENCES

Arcanjo, A.A., Tibiriçá, C.B., Ribatski, G., 2010. "Evaluation of flow patterns and elngated bubble characteristics during the flow boiling of halocarbon refrigerants in micro-scale channel". Experimental Thermal and Fluid Science, Vol. 34, p. 766-775.

Barnea, D., Luninski, Y., Taitel, Y., 1983, Flow pattern in horizontal and vertical two phase flow in small diameter pipe". Can. J. Chem. Eng. Vol. 61, p. 617-620.

Bertsch, S.S., Groll, A.E., Garimella, S.V., 2009, "A composite heat transfer correlation for saturated flow boiling in small channels". Journal of Heat Transfer, Vol. 52, p. 2110 - 2118.

Cheng, P., Wu, H., 2006. "Mesoscale and microscale phase-change heat transfer". Advances in Heat Transfer. Vol. 39, p. 469–573.

Copetti, J.B., Macagnan, M.H., Zinani, Z., Kunsler, N.L.F, 2011, "Flow boiling heat transfer and pressure drop of R-134a in a mini tube:an experimental investigation". Experimental Thermal and Fluid Science Vol. 35, p. 636–644.

Copetti, J.B., Macagnan, M.H., Zinani, Z., 2013, "Experimental study on R-600a boiling in 2.6 mm tube". International Journal of Refrigeration. Vol. 36, p. 325-334.

Felcar, H.O.M., Ribatski, G., Saiz Jabardo, J.M., 2007, "A gas-liquid flow pattern predictive method for macro and mini scale round channels". Proceedings of the 10th UK Heat Transfer Conference. Edinburg, Scotland.

Kandlikar, S.G., 2010, "Scale effects on flow boiling in microchannels: a fundamental perspective". International Journal of Thermal Sciences, Vol. 49, p. 1073-1085.

Kew, P.A. Cornwell, K., 2001. "Correlations for prediction of boiling heat transfer in small – diameter channels". Applied Thermal Engineering Vol. 17-A, p.705-715.

Lazarek, G.M. Black, S.H., 1982. "Evaporative heat transfer, pressure drop and critical heat flux in a small vertical tube with R-113". International Journal of Heat and Mass Transfer, Vol. 25, p.945-960.

Lin, S., Kew, P.A., Cornwell, K., 2001. "Two-phase heat transfer to a refrigerant in a 1 mm diameter tube". International Journal of Refrigeration, Vol. 24, p.51-56.

Ong, C.L., Thome, J.R., 2009. "Flow boiling heat transfer of R134a, R236fa and R245fa in a horizontal 1.030 mm circular channel". Experimental Thermal and Fluid Science, Vol. 33, p. 651-663.

Ong, C.L., Thome, J.R., 2011. "Macro-to-microchannel transition in two-phase flow: Part 1 – Two-phase flow patterns and film thickness measurements". Experimental Thermal and Fluid Science, Vol. 35, p. 37–47.

Revellin, R., Thome, J.R., 2007. "A new type of adiabatic flow pattern map for boiling heat transfer in microchannels". Journal of Micromechanics and Microengineering, Vol. 17, p. 788-796.

Ribatski, G., 2012. "A critical overview on the recent literature concenerning flow boiling and two- phase flows inside microscale channels". In Proceedings of the 8th International Conference on Boiling and Condensation Heat Transfer. Lausanne, Switzerland.

Saitoh, S., Daiguji, H., Hihara, E., 2005. "Effect of tube diameter on boiling heat transfer of R-134a in horizontal small-diameter tubes". International Journal of Heat and Mass Transfer, Vol. 48, p. 4973-4984.

Shiferaw, D., Huo, X., Karayiannis, T.G., Kenning, D.B.R., 2007. "Examination of heat transfer and a model for flow boiling of R134a in small diameter tubes". International Journal of Heat and Mass Transfer, Vol. 50, p. 5177-5193.

Taitel, Y., Dukler, A., 1976, "A model for predicting flow regime transitions in horizontal and near horizontal gas–liquid flow". AIChE Journal Vol. 22, p.47–55.

Thome, J.R., Dupont, V., Jacobi, A.M., 2004, "Heat transfer model for evaporation in microchannels. Part I: presentation of the model". International Journal of Heat and Mass Transfer, Vol.47, p.3375–3385.

Tibiriçá, C.B., Ribatski, G., 2010. "Flow boiling heat transfer of R134a and R245fa in a 2.3 mm tube". International Journal of Heat and Mass Transfer, Vol. 53, p. 2459-2468.

Tran, T.N., Wambsganss, M.W., France, D.M., 1996. "Small circular- and rectangular-channel boiling with two refrigerants". International Journal of Multiphase Flow, Vol. 22, p. 485-498.

Ullmann, A., Brauner, N., 2007, "The prediction of flow pattern maps in minichannels". Multiphase Science and Technology, Vol. 19, No. 1, pp. 49–73.

Wambsganss, M.W., France, D.M., Jendrzejczyk, J.A., Tran, T.N., 1993. "Boiling heat transfer in a horizontal small-diameter tube". Journal of Heat Transfer, Vol. 115, p. 963-972.

Wojtan, L., Ursenbacher, T., Thome, J.R., 2005. "Investigation of flow boiling in horizontal tubes: Part I – A new diabatic two-phase flow pattern map". International Journal of Heat and Mass Transfer, Vol. 48. P. 2955-2969.

Yang, C.C., Shieh, C.C., 2001. "Flow pattern of air-water and two-phase R134a in small circular tubes". International Journal of Heat and Fluid Flow, Vol.27, p. 1163-1177.

Yan, Y.-Y. , Lin, T.-F., 1998. "Evaporation heat transfer and pressure drop of refrigerant R-134a in a small pipe". International Journal of Heat and Mass Transfer, Vol.41, p. 4183-4194.

5. RESPONSIBILITY NOTICE